Spatial correlation functions of inhomogeneous random electromagnetic fields

Luk R. Arnaut*
National Physical Laboratory, Division of Enabling Metrology, Hampton Road, Teddington TW11 0LW, United Kingdom
(Received 31 October 2005; published 7 March 2006)

We analyze the influence of an infinite planar perfectly conducting surface on the spatial correlation functions of a random quasimonochromatic classical electromagnetic vector field, based on a TE/TM decomposition of an angular spectrum of random plane waves. The presence of the surface causes the correlation to depend on both the absolute and relative locations of the field points (inhomogeneous correlation). Known asymptotic results for statistically homogeneous random free fields are retrieved as special cases. The analytical results are illustrated with computations for separations that are either perpendicular or parallel to the surface. The correlation distance for any field component exhibits a damped oscillatory dependency on the local center point. A geometric interpretation in terms of fluctuations of correlation cells is given.

DOI: 10.1103/PhysRevE.73.036604 PACS number(s): 03.50.De, 02.50.−r, 41.20.−q, 05.10.Gg

I. INTRODUCTION

Spatial correlation governs the statistical geometric structure of random fields in terms of the two-point statistical interdependence. Previous studies of spatial correlation functions for stochastic electromagnetic (EM) fields have primarily concentrated on the spatial correlation of free fields (i.e., in homogeneous infinite space), based on space-time [1–3] or analytic [4] characterization of the real or complex electric field, respectively, or in the space-frequency domain for quasimonochromatic fields (e.g., [5]). This idealized situation of an unbounded medium applies to blackbody radiation in thermal equilibrium, serving as an approximation for a wide variety of real or conceptual scenarios at relatively short wavelengths.

More recently, studies of the first-order and second-order statistics of scalar wave fields inside two-dimensional (2D) quantum billiards were reported [6,7]. The close agreement between theoretical predictions for the statistics of quantum wave functions or correlations in chaotic cavities and those measured in 2D nonintegrable microwave resonators [3] suggests an intimate relationship between results from quantum theory and those for wave functions in classical electromagnetism, at least for scalar field components. The suggested relation between quantum chaos for scalar [8] and classical EM random vector fields in three dimensions [9] awaits further investigation. Related studies have analyzed the effect of relative scales of the separation distance on the spatial correlation functions of quantum systems [6,10].

The presence of a physical boundary causes departures of the physical properties of an ideal random field from those in free space, by rendering the local stochastic field to become statistically inhomogeneous and, hence, anisotropic (but not necessarily vice versa [11]). As will be shown, a similar inhomogeneity and anisotropy emerges with regard to the spatial correlation of the field. The effect can be studied through canonical configurations. As a basic example, here we analyze the effect of a perfect electrically conducting (PEC) infinite planar boundary on the spatial correlation function of a random time-harmonic (quasimonochromatic) classical EM field. This simple configuration is of fundamental interest in numerous applications, e.g., in studies of the effect of reflections from the ionosphere, Earth's surface, or natural or man-made obstacles on multipath propagation and correlation of wideband radio waves in otherwise "open" (nonresonant) environments; in scattering from random rough surfaces; for boundary fields in enclosed resonant environments (cavities) such as static chaotic cavities (billiards) [8,9,12], microwave ovens and mode-stirred reverberant (overmoded) cavities, e.g., [13–15]; in coupling of interior to exterior fields through apertures; in EM properties of mesoscopic systems with relatively few degrees of freedom; etc.

Experiments and theoretical analyses have shown that the presence of walls leads to a quantifiable increase of the statistical anisotropy of the interior EM field inside an overmoded cavity [15–18]. More generally, the field in the vicinity of a boundary exhibits departures in its first-order (i.e., local distributional) statistical properties compared to the idealized characteristics of the "deep" field, i.e., at electrically large distances from the nearest boundary [19]. The present theoretical study is a natural extension to second-order (correlation) properties for a particular class of inhomogeneous anisotropic vector EM fields. As will be shown, a major consequence of the ensuing inhomogeneity of the spatial autocorrelation is the fluctuation of the localized correlation distance. The resulting variations in the equivalent number of statistically independent sample points affect the sample statistics. In effect, this number becomes itself a random variable as a function of location. Thus, the effect of statistical field inhomogeneity on its *sample* distributions and associated statistics is twofold (bivariate), viz., through changes in both first-order and second-order properties.

As basic tools for our analysis, we shall here be using the two-point coherence and correlation functions. An alternative approach considers the geometry of nodal lines [20], yielding sharper but more restrictive information about the spatial structure of the field. In an infinite stationary homogeneous lossless medium, an ideal random EM field is statistically homogeneous (quasistationary), i.e., its statistical properties are independent of the absolute location of the space and

*Corresponding author. Electronic address: luk.arnaut@npl.co.uk

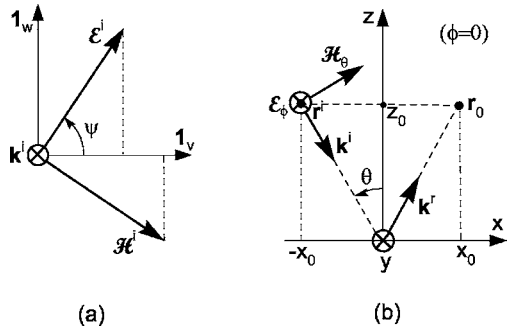

FIG. 1. (a) Local transverse plane; (b) local plane of incidence ($\phi=0$) for single TE component.

time origins. Typically, the degree of statistical field anisotropy and inhomogeneity increases as the location(s) of observation approach(es) a conducting boundary surface, resulting in statistics that depend on the absolute location(s). More generally, dynamic modulation or nonperiodicity of the excitation field in a mechanically static configuration, or time-harmonic excitation in a time-varying configuration [21], leads to spatiotemporal field inhomogeneity and correlation structure.

II. TE/TM DECOMPOSITION OF RANDOM PLANE-WAVE SPECTRUM

For random fields in infinite or semi-infinite spaces, the electric field $\mathbf{E}^i(\mathbf{r})$ generated by time-harmonic sources at infinity within a spherical sector of solid angle Ω can be characterized by a continuous angular spectrum of incident random plane waves as [22] (cf. also [23])

$$\mathbf{E}^i(\mathbf{r}) = \frac{1}{\Omega}\int\int_{\Omega} \mathcal{E}^i(\Omega)\exp(-j\mathbf{k}^i\cdot\mathbf{r})\mathrm{d}\Omega. \tag{1}$$

Here, $\mathcal{E}^i=\mathcal{E}_0\cos\psi\mathbf{1}_v+\mathcal{E}_0\sin\psi\mathbf{1}_w$ with $0\leqslant\psi<\pi$, in which $\mathbf{1}_v$ and $\mathbf{1}_w$ are orthogonal unit vectors spanning the local transverse plane that is orthogonal to the incident wave vector $\mathbf{k}^i$, where $|\mathbf{k}^i|\triangleq k$ is constant (assumption of quasimonochromaticity), and we choose $\mathbf{1}_v\triangleq\mathbf{1}_\phi$, $\mathbf{1}_w\triangleq-\mathbf{1}_\theta$, where $\triangleq$ denotes a definition. The vector spectral amplitude $\mathcal{E}_0$ is a circular complex variate, and ψ is a random orientation angle in the transverse plane with reference to $\mathbf{1}_v$ [Fig. 1(a)]. A standard spherical coordinate system with elevation $(\pi/2)-\theta$ and azimuth ϕ is assumed. A harmonic time dependence $\exp(j\omega t)$ is suppressed throughout.

For each spectral plane-wave component $(\mathcal{E}^i,\mathcal{H}^i,\mathbf{k}^i)$, the propagation and recombination of the incident field with its reflection from an infinite planar impedance boundary is governed by the usual laws for deterministic plane waves. Specifically, consider the transverse electric [(TE) perpendicularly polarized] component of a wave obliquely incident at an angle θ with respect to the positive normal $\mathbf{1}_z$ to the boundary [Fig. 1(b)]. For arbitrary $\mathbf{k}^i$, the plane of incidence for a specific spectral component is spanned by $\mathbf{k}^i$ and $\mathbf{1}_z$, which defines the associated coordinate plane oxz, i.e., $\phi=0$. The incident electric and magnetic fields at an arbitrary location $\mathbf{r}^i(-x_0,z_0)$ with $-x_0\leqslant 0$, $z_0\geqslant 0$, propagating in the direction of $\mathbf{k}^i=k\sin\theta\cos\phi\mathbf{1}_x+k\sin\theta\sin\phi\mathbf{1}_y-k\cos\theta\mathbf{1}_z$, $\forall 0\leqslant\theta<\pi/2$ with $\phi=0$, before reflection, are

$$\mathcal{E}^i_\perp\exp(-j\mathbf{k}^i\cdot\mathbf{r}^i) = \mathcal{E}_0\cos\psi\exp(jkx_0\sin\theta) \times\exp(jkz_0\cos\theta)\mathbf{1}_y, \tag{2}$$

$$\mathcal{H}^i_\perp\exp(-j\mathbf{k}^i\cdot\mathbf{r}^i) = \frac{\mathcal{E}_0}{\eta_0}\cos\psi\exp(jkx_0\sin\theta) \times\exp(jkz_0\cos\theta)[\cos\theta\mathbf{1}_x+\sin\theta\mathbf{1}_z], \tag{3}$$

where $\eta_0\triangleq\sqrt{\mu_0/\epsilon_0}$ is the intrinsic impedance of free space, $\cos\psi=\mathbf{1}_v\cdot\mathcal{E}^i/\mathcal{E}_0$ with $\mathbf{1}_v=\mathbf{1}_y$ and $\mathbf{1}_w=-\cos\theta\mathbf{1}_x-\sin\theta\mathbf{1}_z$.

For specular reflection, the wave vector of the reflected wave is $\mathbf{k}^r=(\underline{\underline{\mathbf{I}}}-2\mathbf{1}_z\mathbf{1}_z)\cdot\mathbf{k}^i=k\sin\theta\mathbf{1}_x+k\cos\theta\mathbf{1}_z$, where $\underline{\underline{\mathbf{I}}}$ symbolizes the unit 3×3 dyadic. The resultant electric field $\mathcal{E}_\perp=\mathcal{E}_{\perp,y}\mathbf{1}_y$ at $\mathbf{r}_0(x_0,z_0)=(\underline{\underline{\mathbf{I}}}-2\mathbf{1}_x\mathbf{1}_x)\cdot\mathbf{r}^i$ follows as $\mathcal{E}^i_\perp(\mathbf{r}_0)+\mathcal{E}^r_\perp(\mathbf{r}_0)=[1+\Gamma_\perp(\theta)]\mathcal{E}^i_\perp(\mathbf{r}_0)$, in which $\mathcal{E}^i_\perp(\mathbf{r}_0)=\mathcal{E}^i_\perp(\mathbf{r}^i)\exp(-j2kx_0\sin\theta)$. The corresponding magnetic field is $\mathcal{H}_\perp=(\mathcal{H}^i_{\perp,x}-\mathcal{H}^r_{\perp,x})\mathbf{1}_x+(\mathcal{H}^i_{\perp,z}+\mathcal{H}^r_{\perp,z})\mathbf{1}_z\triangleq\mathcal{H}_{\perp,x}\mathbf{1}_x+\mathcal{H}_{\perp,z}\mathbf{1}_z$. In case of a PEC boundary $[\Gamma_\perp(\theta)=-1,\forall\theta]$, the dependence of the spectral components of $\mathbf{E}_\perp\equiv\mathbf{E}^i_\perp+\mathbf{E}^r_\perp$ and $\mathbf{H}_\perp\equiv\mathbf{H}^i_\perp+\mathbf{H}^r_\perp$ on $kz_0\cos\theta$ is sinusoidal:

$$\mathcal{E}_\perp\exp(-j\mathbf{k}\cdot\mathbf{r}_0) = j2\mathcal{E}_0\cos\psi\exp(-jkx_0\sin\theta) \times\sin(kz_0\cos\theta)\mathbf{1}_y, \tag{4}$$

$$\mathcal{H}_\perp\exp(-j\mathbf{k}\cdot\mathbf{r}_0) = 2\frac{\mathcal{E}_0}{\eta_0}\cos\psi\exp(-jkx_0\sin\theta) \times[\cos\theta\cos(kz_0\cos\theta)\mathbf{1}_x + j\sin\theta\sin(kz_0\cos\theta)\mathbf{1}_z]. \tag{5}$$

Similarly, the transverse magnetic [(TM) parallel polarized] components of the incident wave are characterized by $\mathcal{H}^i_\parallel=\mathcal{H}^i_{\parallel,y}\mathbf{1}_y$ and $\mathcal{E}^i_\parallel=\mathcal{E}^i_{\parallel,x}\mathbf{1}_x+\mathcal{E}^i_{\parallel,z}\mathbf{1}_z$ with

$$\mathcal{H}^i_\parallel\exp(-j\mathbf{k}^i\cdot\mathbf{r}^i) = \mathcal{H}_0\sin\psi\exp(jkx_0\sin\theta) \times\exp(jkz_0\cos\theta)\mathbf{1}_y, \tag{6}$$

$$\mathcal{E}^i_\parallel\exp(-j\mathbf{k}^i\cdot\mathbf{r}^i) = -\eta_0\mathcal{H}_0\sin\psi\exp(jkx_0\sin\theta) \times\exp(jkz_0\cos\theta)[\cos\theta\mathbf{1}_x+\sin\theta\mathbf{1}_z], \tag{7}$$

with $\sin\psi=\mathbf{1}_v\cdot\mathcal{H}^i/\mathcal{H}_0$, where $\mathcal{H}_0\equiv|\mathcal{H}^i|$. For the resultant fields, $\mathcal{H}_\parallel=(\mathcal{H}^i_{\parallel,y}+\mathcal{H}^r_{\parallel,y})\mathbf{1}_y$ and $\mathcal{E}_\parallel=(\mathcal{E}^i_{\parallel,x}+\mathcal{E}^r_{\parallel,x})\mathbf{1}_x+(\mathcal{E}^i_{\parallel,z}-\mathcal{E}^r_{\parallel,z})\mathbf{1}_z$ at $\mathbf{r}_0$ in case of a PEC surface $[\Gamma_\parallel(\theta)=-1]$, we have

$$\mathcal{H}_\parallel\exp(-j\mathbf{k}\cdot\mathbf{r}_0) = 2\mathcal{H}_0\sin\psi\exp(-jkx_0\sin\theta) \times\cos(kz_0\cos\theta)\mathbf{1}_y, \tag{8}$$

$$\mathcal{E}_\parallel\exp(-j\mathbf{k}\cdot\mathbf{r}_0) = -2\eta_0\mathcal{H}_0\sin\psi\exp(-jkx_0\sin\theta) \times[j\cos\theta\sin(kz_0\cos\theta)\mathbf{1}_x + \sin\theta\cos(kz_0\cos\theta)\mathbf{1}_z]. \tag{9}$$

In summary, for each random plane-wave spectral component $(\mathcal{E}^i, \mathcal{H}^i, \mathbf{k}^i)$ with arbitrary $\mathbf{1}_{k^i}$ and with random ψ and $\mathcal{E}_0$ or $\mathcal{H}_0$, Eqs. (4), (5) and (8), (9) define a pair of TE and TM modal components of the resultant (i.e., incident plus reflected) random fields $\mathbf{E}(\mathbf{r}_0)$ and $\mathbf{H}(\mathbf{r}_0)$, with respect to the plane of incidence $\phi=0$.

For general ϕ, the Cartesian components of a spectral component of $\mathbf{E}(\mathbf{r}_0)=\Omega^{-1}\int\int_\Omega \mathcal{E}(\Omega)\exp(-j\mathbf{k}\cdot\mathbf{r}_0)d\Omega$ and $\mathbf{H}(\mathbf{r}_0)=\Omega^{-1}\int\int_\Omega \mathcal{H}(\Omega)\exp(-j\mathbf{k}\cdot\mathbf{r}_0)d\Omega$, with respect to a fixed reference frame $oxyz$ are, therefore,

$$\mathcal{E}_x \exp(-j\mathbf{k}\cdot\mathbf{r}_0) = j2(\mathcal{E}_\theta \cos\theta\cos\phi - \mathcal{E}_\phi \sin\phi) \times\exp(-jk\varrho_0 \sin\theta)\sin(kz_0\cos\theta), \tag{10}$$

$$\mathcal{E}_y \exp(-j\mathbf{k}\cdot\mathbf{r}_0) = j2(\mathcal{E}_\theta \cos\theta\sin\phi + \mathcal{E}_\phi \cos\phi) \times\exp(-jk\varrho_0 \sin\theta)\sin(kz_0\cos\theta), \tag{11}$$

$$\mathcal{E}_z \exp(-j\mathbf{k}\cdot\mathbf{r}_0) = 2\mathcal{E}_\theta \sin\theta\exp(-jk\varrho_0 \times\sin\theta)\cos(kz_0\cos\theta), \tag{12}$$

where $\varrho_0 \triangleq x_0\cos\phi + y_0\sin\phi$, $\mathcal{E}(\Omega)=\mathcal{E}_\phi\mathbf{1}_\phi+\mathcal{E}_\theta\mathbf{1}_\theta$, $\mathcal{E}_\phi=\mathcal{E}_0\cos\psi$, $\mathcal{E}_\theta=-\eta_0\mathcal{H}_0\sin\psi$ with now $\mathcal{H}_0=\mathcal{E}_0/\eta_0$, and

$$\mathcal{H}_x \exp(-j\mathbf{k}\cdot\mathbf{r}_0) = 2(\mathcal{H}_\theta \cos\theta\cos\phi - \mathcal{H}_\phi \sin\phi) \times\exp(-jk\varrho_0 \sin\theta)\cos(kz_0\cos\theta), \tag{13}$$

$$\mathcal{H}_y \exp(-j\mathbf{k}\cdot\mathbf{r}_0) = 2(\mathcal{H}_\theta \cos\theta\sin\phi + \mathcal{H}_\phi \cos\phi) \times\exp(-jk\varrho_0 \sin\theta)\cos(kz_0\cos\theta), \tag{14}$$

$$\mathcal{H}_z \exp(-j\mathbf{k}\cdot\mathbf{r}_0) = j2\mathcal{H}_\theta \sin\theta\exp(-jk\varrho_0 \times\sin\theta)\sin(kz_0\cos\theta), \tag{15}$$

with $\mathcal{H}(\Omega)=\mathcal{H}_\phi\mathbf{1}_\phi+\mathcal{H}_\theta\mathbf{1}_\theta$, $\mathcal{H}_\theta=(\mathcal{E}_0/\eta_0)\cos\psi$, $\mathcal{H}_\phi=\mathcal{H}_0\sin\psi$. Except in Sec. III D, we shall further consider the correlation properties of the electric field only; corresponding properties for the magnetic field follow *mutatis mutandis*.

III. SEPARATION IN NORMAL DIRECTION

A. Tangential field

For the calculation of the two-point spatial correlation, the quantity of fundamental importance is the 3×3 field coherency dyadic $\langle\mathbf{E}(\mathbf{r}_1)\mathbf{E}^*(\mathbf{r}_2)\rangle$ at arbitrary locations $\mathbf{r}_1$ and $\mathbf{r}_2$ [4]. For separation in normal direction ($x_1=x_2\triangleq0$ and $y_1=y_2\triangleq0$), the azimuthal symmetry can be exploited from which the general solution can be constructed from the TE and TM components.

For TE components, from (1) and (4), i.e., (11) with $\phi=0$,

$$\langle E_y(x_1,z_1)E_y^*(x_2,z_2)\rangle = \frac{1}{\Omega_1\Omega_2}\Bigg\langle \int\int_{\Omega_1}\int\int_{\Omega_2} [j2\mathcal{E}_1(\Omega_1) \times\exp(-jkx_1\sin\theta_1)\sin(kz_1\cos\theta_1)] \times[-j2\mathcal{E}_2^*(\Omega_2)\exp(jkx_2\sin\theta_2) \times\sin(kz_2\cos\theta_2)]d\Omega_2 d\Omega_1\Bigg\rangle, \tag{16}$$

where $\langle\cdot\rangle$ denotes ensemble averaging and $d\Omega_{1,2}=\sin\theta_{1,2}d\phi_{1,2}d\theta_{1,2}$ for the angular ranges $0\leqslant\phi_{1,2}<2\pi$ and $0\leqslant\theta_{1,2}<\pi/2$, i.e., integration and normalization are with respect to the half space of the source field ($\Omega_{1,2}=2\pi$ sr). Since $\langle\mathrm{Re}[\mathcal{E}_{p_\alpha}]\mathrm{Im}[\mathcal{E}_{q_\beta}]\rangle=0$ for an ideal random field, and on account of $\mathcal{E}_{m_y}=\mathcal{E}_{m_\phi}\mathbf{1}_\phi$ for TE polarization (α, $\beta=\phi$ or θ; m, $p,q=1,2$), by definition of $\mathbf{1}_\phi\equiv\mathbf{1}_y$, we have for circular $\mathcal{E}_m$,

$$\begin{aligned}\langle\mathcal{E}_1(\Omega_1)\cdot\mathcal{E}_2^*(\Omega_2)\rangle &= \langle\mathcal{E}_{1_\theta}(\Omega_1)\mathcal{E}_{2_\theta}^*(\Omega_2)\rangle + \langle\mathcal{E}_{1_\phi}(\Omega_1)\mathcal{E}_{2_\phi}^*(\Omega_2)\rangle \\ &= \langle\mathrm{Re}[\mathcal{E}_{1_\phi}(\Omega_1)]\mathrm{Re}[\mathcal{E}_{2_\phi}(\Omega_2)]\rangle \\ &\quad + \langle\mathrm{Im}[\mathcal{E}_{1_\phi}(\Omega_1)]\mathrm{Im}[\mathcal{E}_{2_\phi}(\Omega_2)]\rangle \\ &= 2C\delta(\Omega_{12}),\end{aligned} \tag{17}$$

where $C\triangleq\langle|\mathcal{E}_0|^2\rangle/4$, $\Omega_{12}\triangleq(\Omega_1\cup\Omega_2)\backslash(\Omega_1\cap\Omega_2)$ and Kronecker's delta for sets is here defined by $\delta(\emptyset)\triangleq1$, valid when both solid angles completely overlap ($\Omega_1=\Omega_2$), but equaling 0 for any other nonempty sets Ω_{12} (i.e., for $\Omega_1\neq\Omega_2$). On substituting (17) into (16), and accounting for the assumption $x_1=x_2$,

$$\begin{aligned}\langle E_y(x_1,z_1)E_y^*(x_1,z_2)\rangle &= \frac{8C}{2\pi}\int_0^{2\pi}d\phi\int_0^{\pi/2}\exp[-jk(x_1 \\ &\quad - x_2)\sin\theta]_{x_1=x_2}\sin(kz_1\cos\theta) \\ &\quad \times\sin(kz_2\cos\theta)\sin\theta d\theta \\ &= 4C\{\mathrm{sinc}[k(z_1-z_2)] - \mathrm{sinc}[k(z_1+z_2)]\}.\end{aligned} \tag{18}$$

The spatial autocorrelation function of E_y follows as:

$$\rho_{E_y}(z_1,z_2) \triangleq \frac{\langle E_y(z_1)E_y^*(z_2)\rangle}{\sqrt{\langle|E_y(z_1)|^2\rangle\langle|E_y(z_2)|^2\rangle}} \tag{19}$$

$$= \frac{\mathrm{sinc}[k(z_1-z_2)] - \mathrm{sinc}[k(z_1+z_2)]}{\sqrt{1-\mathrm{sinc}(2kz_1)}\sqrt{1-\mathrm{sinc}(2kz_2)}}. \tag{20}$$

Thus, the presence of a PEC surface results in $\rho_{E_y}(z_1,z_2)$—like $E_y(z)$ itself—becoming inhomogeneous, i.e., its value depends now also on the absolute distances $z_{1,2}$, in addition to the familiar dependence on the separation $\Delta z=|z_1-z_2|$ for homogeneous spatial correlation in unbounded space (cf. Sec. II of [1]). The result (20) is to be compared with the functional $\mathrm{sinc}[f(z_1-z_2,z_1+z_2)]$ in Eq. (21) of [24] for the case of localized random functions. For the asymptotically deep field, i.e., for $\min(kz_1,kz_2)\to+\infty$,

$$\rho_{E_y}(z_1,z_2) \to \mathrm{sinc}[k(z_1-z_2)]. \tag{21}$$

This expression differs, of course, from the one for the transverse field in unbounded space [cf. (29)], because (21) contains contributions by TE components only. In the spectral expansion, the contribution by the E_x of TM vector components must also be accounted for. On the other hand, for TE waves, E_y constitutes the total field, in which case (21) corresponds to the asymptotic correlation function for the vector field in unbounded space (cf. Sec. III C).

For TM wave components, the correlation functions for E_x and E_z are obtained in a similar manner. With now $\mathcal{E}_m = -\mathcal{E}_{m_\theta}\mathbf{1}_\theta$, from (9),

$$\langle E_x(z_1)E_x^*(z_2)\rangle = 4C\int_0^1 \exp[-jk(x_1-x_2)\sqrt{1-u^2}]_{x_1=x_2} \times \{\cos[k(z_1-z_2)u] - \cos[k(z_1+z_2)u]\}u^2du \tag{22}$$

$$= 4C\left\{\mathrm{sinc}[k(z_1-z_2)] - \frac{2\sin[k(z_1-z_2)]}{[k(z_1-z_2)]^3} + \frac{2\cos[k(z_1-z_2)]}{[k(z_1-z_2)]^2} - \mathrm{sinc}[k(z_1+z_2)] + \frac{2\sin[k(z_1+z_2)]}{[k(z_1+z_2)]^3} - \frac{2\cos[k(z_1+z_2)]}{[k(z_1+z_2)]^2}\right\}, \tag{23}$$

in which $u \triangleq \cos\theta$. In particular, when $z_1 = z_2$,

$$\langle |E_x(z_{1,2})|^2\rangle = 4C\left[\frac{1}{3} - \mathrm{sinc}(2kz_{1,2}) + \frac{2\sin(2kz_{1,2})}{(2kz_{1,2})^3} - \frac{2\cos(2kz_{1,2})}{(2kz_{1,2})^2}\right]. \tag{24}$$

The explicit expression for $\rho_{E_x}(z_1,z_2) \triangleq \langle E_x(z_1)E_x^*(z_2)\rangle / \sqrt{\langle |E_x(z_1)|^2\rangle\langle |E_x(z_2)|^2\rangle}$ follows upon substituting (23) and (24) herein.

For the correlation function of the tangential field E_t, parallel to the surface, the contributions by the TE and TM waves are to be combined. Since such pairs of modal field components are mutually orthogonal and uncorrelated, i.e., $\langle \mathrm{Re}[\mathcal{E}_\alpha]\mathrm{Re}[\mathcal{E}_\beta^*]\rangle = \langle \mathrm{Im}[\mathcal{E}_\alpha]\mathrm{Im}[\mathcal{E}_\beta^*]\rangle = \langle \mathrm{Re}[\mathcal{E}_\alpha]\mathrm{Im}[\mathcal{E}_\beta^*]\rangle = 0$, and because of the azimuthal symmetry of the configuration,

$$\langle E_t(z_1)E_t^*(z_2)\rangle = \langle E_x(z_1)E_x^*(z_2)\rangle + \langle E_y(z_1)E_y^*(z_2)\rangle. \tag{25}$$

Therefore, we finally arrive at

$$\rho_{E_t}(z_1,z_2) \triangleq \frac{\langle E_t(z_1)E_t^*(z_2)\rangle}{\sqrt{\langle |E_t(z_1)|^2\rangle\langle |E_t(z_2)|^2\rangle}}, \tag{26}$$

with

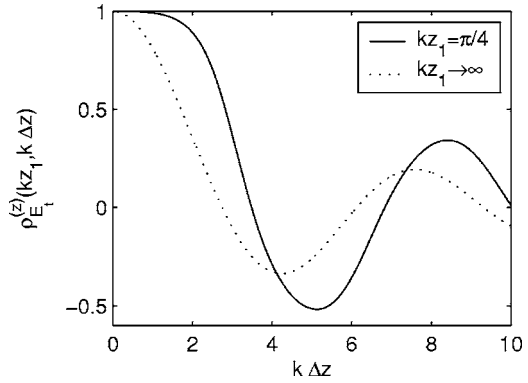

FIG. 2. Spatial correlation function $\rho_{E_t}(kz_1,k\Delta z)$ of tangential field as a function separation $k\Delta z$ in normal direction ($x_1=x_2, y_1=y_2$).

$$\langle E_t(z_1)E_t^*(z_2)\rangle = 8C\left\{\mathrm{sinc}[k(z_1-z_2)] - \frac{\sin[k(z_1-z_2)]}{[k(z_1-z_2)]^3} + \frac{\cos[k(z_1-z_2)]}{[k(z_1-z_2)]^2} - \mathrm{sinc}[k(z_1-z_2)] + \frac{\sin[k(z_1+z_2)]}{[k(z_1+z_2)]^3} - \frac{\cos[k(z_1+z_2)]}{[k(z_1+z_2)]^2}\right\}, \tag{27}$$

$$\langle |E_t(z_{1,2})|^2\rangle = 8C\left[\frac{2}{3} - \frac{\sin(2kz_{1,2})}{2kz_{1,2}} + \frac{\sin(2kz_{1,2})}{(2kz_{1,2})^3} - \frac{\cos(2kz_{1,2})}{(2kz_{1,2})^2}\right]. \tag{28}$$

In the limit $\min(kz_1,kz_2) \to +\infty$, $\rho_{E_t}(z_1,z_2)$ becomes again homogeneous and reduces to the known result for a quasi-monochromatic transverse field in unbounded space [1–3,5,25]

$$\rho_{E_t}(z_1,z_2) \to \frac{3}{2}\left\{\mathrm{sinc}[k(z_1-z_2)] - \frac{\sin[k(z_1-z_2)]}{[k(z_1-z_2)]^3} + \frac{\cos[k(z_1-z_2)]}{[k(z_1-z_2)]^2}\right\}. \tag{29}$$

This correspondence is remarkable, for the deep field in the presence of a PEC plane always originates from a statistically *anisotropic* source field, as incidence is from within a half space ($\Omega_{1,2}=2\pi$ sr), even when $\min(kz_1,kz_2) \to +\infty$ because generating sources for plane waves are located at infinity. In this case, the average power flux density of the incident field is $\langle \mathbf{P}^i(\mathbf{r})\rangle = -[\langle |\mathcal{E}_0|^2\rangle/(4\eta_0)]\mathbf{1}_z$. By contrast, in the absence of a boundary, incidence in unbounded space is from all directions ($\Omega_{1,2}=4\pi$ sr) and is statistically isotropic ($\langle \mathbf{P}^i(\mathbf{r})\rangle = \mathbf{0}$). This suggests that (29) holds only when the boundary is ideal, i.e., infinite, planar, and perfectly conducting, so as to create an ideal image of the source field for which $\langle \mathbf{P}(\mathbf{r})\rangle = \mathbf{0}$.

Figure 2 compares $\rho_{E_t}(kz_1=\pi/4,k\Delta z)$ with $\rho_{E_t}(kz_1$

$\rightarrow +\infty, k\Delta z$), demonstrating the increased correlation for relative small $k\Delta z$ compared to that for the deep or unbounded field. The increase in the distance $k\Delta z$ to the first zero crossing (correlation distance; cf. Sec. V) and the increased amplitude of oscillations now explain at least qualitatively the previously observed discrepancies between theoretical and experimentally measured correlation functions $\rho_{E_t}^{(z)}(kz_1 < \infty, k\Delta z)$ for TM modes of 2D microwave billiards, e.g., in Fig. 2(a) of [3], where comparison with the theoretical result for the deep field (i.e., assuming an arbitrary large distance between the field probe and the nearest short cavity wall) was made instead. Note that here we have introduced the superscript "(z)" indicating explicitly the direction of point separation, for later benefit.

B. Normal field

For the field component E_z, in the direction normal to the boundary, the spatial correlation function

$$\rho_{E_z}(z_1, z_2) \triangleq \frac{\langle E_z(z_1) E_z^*(z_2)\rangle}{\sqrt{\langle |E_z(z_1)|^2\rangle}\sqrt{\langle |E_z(z_2)|^2\rangle}} \tag{30}$$

can be calculated solely from the TM components, using

$$\begin{aligned}\langle E_z(z_1) E_z^*(z_2)\rangle &= 4C\int_0^1 \exp[-jk(x_1 - x_2)\sqrt{1-u^2}]_{x_1=x_2} \\ &\quad \times \{\cos[k(z_1 - z_2)u] + \cos[k(z_1 + z_2)u]\} \\ &\quad \times (1-u^2)du \\ &= 8C\left\{\frac{\sin[k(z_1 - z_2)]}{[k(z_1 - z_2)]^3} - \frac{\cos[k(z_1 - z_2)]}{[k(z_1 - z_2)]^2}\right. \\ &\quad \left. + \frac{\sin[k(z_1 + z_2)]}{[k(z_1 + z_2)]^3} - \frac{\cos[k(z_1 + z_2)]}{[k(z_1 + z_2)]^2}\right\}\end{aligned} \tag{31}$$

with, in particular,

$$\langle |E_z(z_{1,2})|^2\rangle = 8C\left[\frac{1}{3} + \frac{\sin(2kz_{1,2})}{(2kz_{1,2})^3} - \frac{\cos(2kz_{1,2})}{(2kz_{1,2})^2}\right]. \tag{32}$$

When $\min(kz_1, kz_2) \rightarrow +\infty$, we retrieve the known correlation function for the longitudinal field component in an unbounded homogeneous medium [1–3,5,25]

$$\rho_{E_z}(z_1, z_2) \rightarrow 3\left\{\frac{\sin[k(z_1 - z_2)]}{[k(z_1 - z_2)]^3} - \frac{\cos[k(z_1 - z_2)]}{[k(z_1 - z_2)]^2}\right\}. \tag{33}$$

Figure 3 compares $\rho_{E_z}(kz_1 = \pi/4, k\Delta z)$ (solid line) with the asymptotic result $\rho_{E_z}(kz_1 \rightarrow +\infty, k\Delta z)$ (dotted line). Compared to ρ_{E_t}, the effect of the PEC surface on ρ_{E_z} is now significantly weaker. While the correlation for $k\Delta z < 2$ has again increased, the first zero crossing of $\rho_{E_z}(kz_1 = \pi/4, k\Delta z)$ now occurs at smaller values of $k\Delta z$ compared to those for $\rho_{E_z}(kz_1 \rightarrow +\infty, k\Delta z)$.

C. Amplitude of vector field

For the magnitude of the total field, $E \triangleq |\mathbf{E}|$, the contributions of both TE and TM wave components can again be summed, on account of mode orthogonality and configurational symmetry, yielding

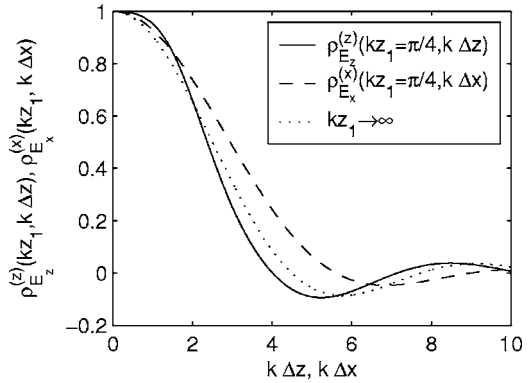

FIG. 3. Spatial correlation functions $\rho_{E_z}^{(z)}(kz_1, k\Delta z)$ and $\rho_{E_x}^{(x)}(kz_1, k\Delta x)$ of longitudinal field as a function of separation $k\Delta z$ in normal direction ($x_1 = x_2, y_1 = y_2$) or $k\Delta x$ in tangential direction ($z_1 = z_2$), respectively. The asymptotic functions are identical, i.e., $\rho_{E_z}^{(z)}(kz_1 \rightarrow +\infty, k\Delta z) = \rho_{E_x}^{(x)}(kz_1 \rightarrow +\infty, k\Delta x)$.

$$\begin{aligned}\langle E(z_1) E^*(z_2)\rangle &= \langle E_x(z_1) E_x^*(z_2)\rangle + \langle E_y(z_1) E_y^*(z_2)\rangle \\ &\quad + \langle E_z(z_1) E_z^*(z_2)\rangle.\end{aligned} \tag{34}$$

With the aid of (18), (23), and (31), we arrive at

$$\rho_E(z_1, z_2) \triangleq \frac{\langle E(z_1) E^*(z_2)\rangle}{\sqrt{\langle |E(z_1)|^2\rangle}\sqrt{\langle |E(z_2)|^2\rangle}}, \tag{35}$$

where

$$\begin{aligned}\langle E(z_1) E^*(z_2)\rangle &= 8C\left\{\mathrm{sinc}[k(z_1 - z_2)] - \mathrm{sinc}[k(z_1 + z_2)]\right. \\ &\quad \left. + \frac{2\sin[k(z_1 + z_2)]}{[k(z_1 + z_2)]^3} - \frac{2\cos[k(z_1 + z_2)]}{[k(z_1 + z_2)]^2}\right\},\end{aligned}$$

$$\begin{aligned}\langle |E(z_{1,2})|^2\rangle &= 8C\left[1 - \mathrm{sinc}(2kz_{1,2}) + \frac{2\sin(2kz_{1,2})}{(2kz_{1,2})^3}\right. \\ &\quad \left. - \frac{2\cos(2kz_{1,2})}{(2kz_{1,2})^2}\right].\end{aligned} \tag{36}$$

If $\min(kz_1, kz_2) \rightarrow +\infty$, then (35) approaches the result for statistically homogeneous free fields [2], i.e.,

$$\rho_E(z_1, z_2) \rightarrow \mathrm{sinc}[k(z_1 - z_2)], \tag{37}$$

as expected by now.

Figure 4 compares $\rho_E(kz_1 = \pi/4, k\Delta z)$ (solid line) with $\rho_E(kz_1 \rightarrow +\infty, k\Delta z)$ (dotted line). Qualitatively, the effect of E_t on ρ_E is seen to dominate the contribution of E_z.

From (28), (32), and (33), it follows that the energy density becomes statistically homogeneous when $\min(kz_1, kz_2) \rightarrow +\infty$, despite the presence of the PEC plane: standing waves of individual modes do not persist, owing to the randomness of the field.

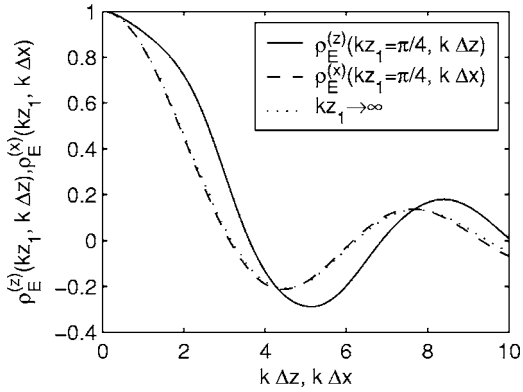

FIG. 4. Spatial correlation functions $\rho_E^{(z)}(kz_1,k\Delta z)$ and $\rho_E^{(x)}(kz_1,k\Delta x)$ of the total field as a function of separation $k\Delta z$ in normal direction $(x_1=x_2,y_1=y_2)$ or $k\Delta x$ in tangential direction $(z_1=z_2)$, respectively. The asymptotic functions are identical.

D. Different and mixed field components

Finally, the mixed-correlation functions [4] between different field components are obtained *mutatis mutandis*. For components belonging to different modal types (one TE, one TM), the correlation is zero because of mode orthogonality. For components belonging to the same TM mode, however,

$$\rho_{E_xE_z}(z_1,z_2)\triangleq\frac{\langle E_x(z_1)E_z^*(z_2)\rangle}{\sqrt{\langle|E_x(z_1)|^2\rangle\langle|E_z(z_2)|^2\rangle}} \tag{38}$$

with $\langle|E_x(z_1)|^2\rangle$ and $\langle|E_z(z_2)|^2\rangle$ given by (24) and (32), respectively, and with

$$\langle E_x(z_1)E_z^*(z_2)\rangle=-j8C\left[\frac{J_2[k(z_1-z_2)]}{k(z_1-z_2)}+\frac{J_2[k(z_1+z_2)]}{k(z_1+z_2)}\right], \tag{39}$$

where $J_2(\cdot)$ is the Bessel function of the first kind and second order. The fact that (39) is purely imaginary indicates that E_x and E_z are correlated in phase quadrature as a consequence of the PEC boundary condition, which is apparent from a comparison of (9) with (7). Furthermore, $\rho_{E_xE_z}(z_1,z_2)=\rho^*_{E_zE_x}(z_2,z_1)=\rho_{H_zH_x}(z_1,z_2)$. By contrast, for an arbitrary tangential direction $\mathbf{1}_t$, the electric-electric mixed-correlation function vanishes: $\mathbf{E}_t=E_x\cos\phi\mathbf{1}_x+E_y\sin\phi\mathbf{1}_y$, so that upon substitution, using (39) and ϕ integration across $[0,2\pi]$ with kernel $\cos\phi$ or $\sin\phi$, it follows that $\langle E_t(z_1)E_z^*(z_2)\rangle=0$. Thus, (38) and (39) are only relevant in case of a 2D random field whose spectral components consist of TM modes that all have their $\mathbf{k}^i$ lying within a single plane of incidence (ϕ =constant).

The function $-j\rho_{E_xE_z}(kz_1=\pi/4,k\Delta z)$ is shown in Fig. 5, where it is compared with its asymptotic form for $kz_1\to+\infty$. In the former case, $-j\rho_{E_xE_z}(kz_1,k\Delta z)$ tends to a z_1-dependent negative value when $k\Delta z\to0$, whereas in the latter case, the function tends to zero. Moreover, if $kz_1=kz_2\to0$, then $\rho_{E_xE_z}(kz_1)\simeq-j(\sqrt{30}/8)[1-(2kz_1)^2/35]$.

For the mixed correlation between electric and magnetic field components, from

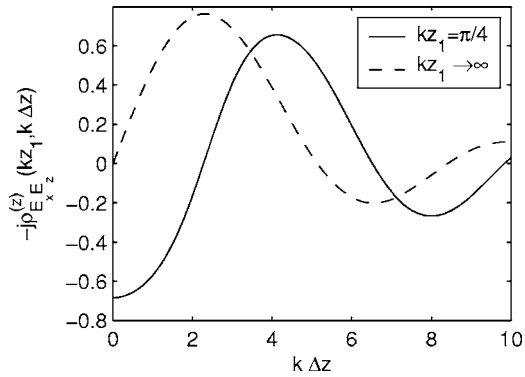

FIG. 5. Mixed spatial correlation function $-j\rho_{E_xE_z}(kz_1,k\Delta z)$ for a 2D TM field as a function of separation $k\Delta z$ in normal direction $(x_1=x_2,\ y_1=y_2)$.

$$\langle E_x(z_1)H_y^*(z_2)\rangle=-\frac{j4C}{\eta_0}\left\{\frac{\sin[k(z_1-z_2)]}{[k(z_1-z_2)]^2}-\frac{\cos[k(z_1-z_2)]}{k(z_1-z_2)}+\frac{\sin[k(z_1+z_2)]}{[k(z_1+z_2)]^2}-\frac{\cos[k(z_1+z_2)]}{k(z_1+z_2)}\right\}, \tag{40}$$

$$\langle H_y(z_1)H_y^*(z_2)\rangle=\frac{4C}{\eta_0^2}\{\mathrm{sinc}[k(z_1-z_2)]+\mathrm{sinc}[k(z_1+z_2)]\}, \tag{41}$$

and, in particular,

$$\langle|H_y(z_2)|^2\rangle=\frac{4C}{\eta_0^2}[1+\mathrm{sinc}(2kz_2)], \tag{42}$$

we obtain $\rho_{E_xH_y}(z_1,z_2)$ by substituting (24), (40), and (42) into (38), after replacing E_z by H_y in the latter definition. Note that $\rho_{E_xH_y}(z_1,z_2)=\rho^*_{E_yH_x}(z_1,z_2)\equiv-\rho_{E_yH_x}(z_1,z_2)$ is purely imaginary and does not vanish for any pair of mutually orthogonal tangential directions. For $\min(kz_1,kz_2)\to+\infty$, we retrieve the known result for unbounded space [25]

$$\rho_{E_xH_y}(z_1,z_2)\to-j\frac{3}{2}\left\{\frac{\sin[k(z_1-z_2)]}{[k(z_1-z_2)]^2}-\frac{\cos[k(z_1-z_2)]}{k(z_1-z_2)}\right\}. \tag{43}$$

Figure 6 compares $-j\rho_{E_xH_y}(kz_1=\pi/4,k\Delta z)$ with its asymptotic form. Unlike for unbounded random fields, orthogonal tangential electric and magnetic components at a single location near the surface $(kz_1\to0)$ are significantly correlated in phase quadrature. This correlation gradually decreases in strength when kz_1 is increased. For $kz_1=kz_2\to0$, $\rho_{E_xH_y}(kz_1)\simeq-j(\sqrt{5}/3)[1-(2kz_1)^2/35]$, i.e., unlike unbounded fields, electric and magnetic field components at the same location in front of a PEC surface show nonvanishing correlation.

For the TM modes of a 2D field that are incident in a single plane,

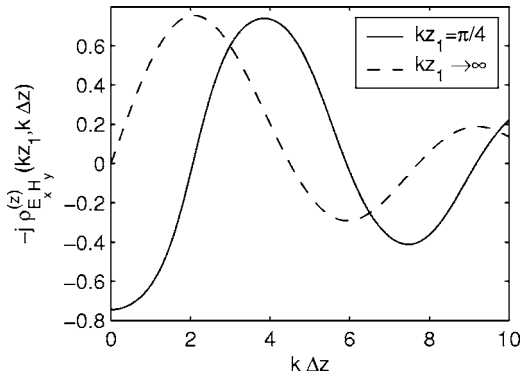

FIG. 6. Mixed spatial correlation function $-j\rho_{E_xH_y}(kz_1,k\Delta z)$ as a function of separation $k\Delta z$ in normal direction ($x_1=x_2$, $y_1=y_2$).

$$\langle E_z(z_1)H_y^*(z_2)\rangle = -j\frac{2\pi C}{\eta_0}\left[\frac{J_1[k(z_1-z_2)]}{k(z_1-z_2)}+\frac{J_1[k(z_1+z_2)]}{k(z_1+z_2)}\right], \tag{44}$$

which again valishes upon integration across the azimuthal plane. Thus, correlation between electric and magnetic three-dimensional fields exists only between their transverse components.

IV. ARBITRARY DIRECTION OF POINT SEPARATION

Consider next two arbitrary locations $\mathbf{r}_1 \neq \mathbf{r}_2$ and a global reference frame $oxyz$ (Fig. 7). Although the general solution can, in principle, be obtained with the aid of (10)–(15), we shall again take advantage of the azimuthal symmetry of the configuration.

Without loss of generality, the projection of the line connecting both locations onto the boundary plane ($z=0$) defines the reference direction ox in the tangential plane, whence $y_1=y_2=0$. The axis ox subtends an angle $\phi \triangleq \widehat{ox', ox}$ with the local plane of incidence $ox'z'$ that is associated with each impinging plane-wave component and spanned by $\mathbf{k}^{i'}$ and $oz' \equiv oz$, whence $\mathbf{k}^{i'} \cdot \mathbf{r}' = kx \sin\theta\cos\phi - kz\cos\theta$. The spectral field components associated with $ox'z'$ are now obtained by replacing x by its projection $x'=x\cos\phi$. With reference to oxz, the tangential field E_x consists of TM contributions $\mathcal{E}_{x'}\cos\phi$ and TE contributions $\mathcal{E}_{y'}\sin\phi$, whereas the tangential transverse field E_y contains TE contributions $\mathcal{E}_{y'}\cos\phi$ and TM contributions $-\mathcal{E}_{x'}\sin\phi$. The normal field $\mathcal{E}_z \equiv \mathcal{E}_{z'}$, being independent of ϕ, still consists of TM contributions only. Hence, for each vector plane-wave component,

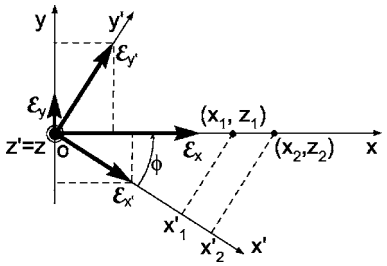

FIG. 7. Local and reference oordinate systems $ox'y'z'$ and $oxyz$ for analysis of arbitrary direction of point separation.

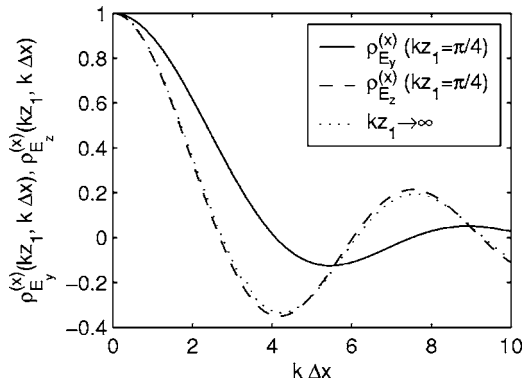

FIG. 8. Spatial correlation functions $\rho_{E_y}(kz_1,k\Delta x)$ and $\rho_{E_z}(kz_1,k\Delta x)$ of transverse field as a function of tangential separation $k\Delta x$ for $z_1=z_2$.

$$\mathcal{E}_x(\mathbf{r}_1)\mathcal{E}_x^*(\mathbf{r}_2) = \mathcal{E}_{x'}(\mathbf{r}_1)\mathcal{E}_{x'}^*(\mathbf{r}_2)\cos^2\phi + \mathcal{E}_{y'}(\mathbf{r}_1)\mathcal{E}_{y'}^*(\mathbf{r}_2)\sin^2\phi + [\mathcal{E}_{x'}(\mathbf{r}_1)\mathcal{E}_{y'}^*(\mathbf{r}_2) + \mathcal{E}_{x'}^*(\mathbf{r}_1)\mathcal{E}_{y'}(\mathbf{r}_2)]\sin\phi\cos\phi \tag{45}$$

$$\mathcal{E}_y(\mathbf{r}_1)\mathcal{E}_y^*(\mathbf{r}_2) = \mathcal{E}_{x'}(\mathbf{r}_1)\mathcal{E}_{x'}^*(\mathbf{r}_2)\sin^2\phi + \mathcal{E}_{y'}(\mathbf{r}_1)\mathcal{E}_{y'}^*(\mathbf{r}_2)\cos^2\phi - [\mathcal{E}_{x'}(\mathbf{r}_1)\mathcal{E}_{y'}^*(\mathbf{r}_2) + \mathcal{E}_{x'}^*(\mathbf{r}_1)\mathcal{E}_{y'}(\mathbf{r}_2)]\sin\phi\cos\phi \tag{46}$$

from which $\mathcal{E}_x(\mathbf{r}_1)\mathcal{E}_x^*(\mathbf{r}_2)+\mathcal{E}_y(\mathbf{r}_1)\mathcal{E}_y^*(\mathbf{r}_2) = \mathcal{E}_{x'}(\mathbf{r}_1)\mathcal{E}_{x'}^*(\mathbf{r}_2) + \mathcal{E}_{y'}(\mathbf{r}_1)\mathcal{E}_{y'}^*(\mathbf{r}_2)$. Integration with respect to θ and ϕ, followed by ensemble averaging, yields again the covariance and correlation functions of E_x and E_y. The mixed-product terms involve both TE and TM components and average to zero because $\langle \mathcal{E}_{x'}\mathcal{E}_{y'}^*\rangle = 0$, so that the bracketed terms in (45) and (46) do not contribute.

As a canonical example, we calculate correlation functions for tangential separation of $\mathbf{r}_1$ and $\mathbf{r}_2$ along a line parallel to the ox axis and at equal height above the boundary ($z_1=z_2>0$, $y_1=y_2=0$), i.e., $\rho_{E_\alpha}^{(x)}(x_1,z_1;x_2,z_1)$. Figures 3, 4, and 8 show results for the longitudinal, total, and transverse field, respectively, as a function of the separation $k\Delta x \equiv k|x_1-x_2|$. The case $kz_1=\pi/4$ is compared with the asymptotic result for $kz_1 \to +\infty$. All three correlation functions are qualitatively similar and show an increased first zero-crossing distance closer to the surface compared to the asymptotic result, as expected. Note that $\rho_{E_z}^{(x)}(kz_1 \to +\infty, k\Delta x) = \rho_{E_x}^{(z)}(kz_1 \to +\infty, k\Delta z)$, but $\rho_{E_t}^{(x)}(kz_1 \to +\infty, k\Delta x) \neq \rho_{E_t}^{(z)}(kz_1 \to +\infty, k\Delta z)$, because $E_t^{(x)}$ involves a mixture of longitudinal and transverse field components, whereas $E_t^{(z)}$ consists solely of transverse components. Instead, $\rho_{E_t}^{(x)}(kz_1 \to +\infty, k\Delta x) = \rho_{E_{yz}}^{(z)}(kz_1 \to +\infty, k\Delta z)$, where $\mathbf{E}_{yz} \triangleq E_y\mathbf{1}_y + E_z\mathbf{1}_z$.

The previous results permit a simple geometrical interpretation. At two arbitrary locations at asymptotically large distances from the surface, the relative instantaneous orientation of the local field phasors $\mathbf{E}(\mathbf{r}_1)$ and $\mathbf{E}(\mathbf{r}_2)$ is governed only

TABLE I. Asymptotic values of correlation length $\ell^{(\alpha)}(kz_1)$ (in units $k\Delta\alpha$) for E_β calculated using (47).

	$\ell^{(z)}(0)$	$\ell^{(z)}(\infty)$	$\ell^{(z)}(0)/\ell^{(z)}(\infty)$	$\ell^{(x)}(0)$	$\ell^{(x)}(\infty)$	$\ell^{(x)}(0)/\ell^{(x)}(\infty)$
E_x	3.870	2.744	1.411	5.535	4.493	1.232
E_y	4.493	2.744	1.638	4.185	2.744	1.525
E_z	4.493	4.493	1.000	2.744	2.744	1.000
E_t	4.233	2.744	1.543			
E	4.493	π	1.430	2.744	π	0.8734

by their relative distance, on account of their asymptotically homogeneous spatial correlation (for example, for a quasi-stationary mode-stirred reverberant field [21], these phasors are slowly and randomly rotating in all three dimensions of configurational space). Their mutual coherence is defined by the ensemble average of the projection (complex scalar product) of one phasor onto the other. When both locations approach a PEC surface with preservation of their mutual distance, both phasors start lining up, as they would also do in the case when their relative distance would be reduced. This alignment becomes more pronounced with decreasing absolute or relative height above the surface and is stronger for field components that are parallel to the surface than for normal fields. On reaching the surface, the values of corresponding field components are completely correlated, irrespective of the separation distance parallel to the surface.

V. CORRELATION DISTANCE

Since the previous correlation functions are either purely real or purely imaginary (on account of the surface being perfectly conducting) and exhibit damped oscillations with respect to their zero asymptotic value, we can define an associated (dimensionless) spatial (auto)correlation distance for E (or for any one of its Cartesian components), as measured in the direction of point separation $\mathbf{1}_\alpha$, based on the first zero-crossing distance of $\rho_E(kz_1, k\Delta\alpha)$

$$\ell^{(\alpha)}(kz_1) \triangleq \rho_E^{-1}(kz_1, 0), \tag{47}$$

where $\alpha = x, y, z$. This definition has the advantage of being simple to calculate to arbitrary precision from $\rho_E(kz_1, k\Delta\alpha)$. Asymptotic values of $\ell^{(\alpha)}(kz_1)$ for $kz_1 \to 0$ and $kz_1 \to +\infty$ corresponding to the definition (47) are listed in Table I. The asymptotic correlation distance $\ell^{(\alpha)}(kz_1 \to +\infty)$ will be further denoted as $\ell_\infty^{(\alpha)}$ for brevity.

Alternatively, the spatial correlation length may be defined as the area

$$\ell^{(\alpha)}(kz_1) \triangleq \int_{-\infty}^{+\infty} |\rho_E(kz_1, k\Delta\alpha)|^2 \mathrm{d}(k\Delta\alpha). \tag{48}$$

This definition has the advantage of being also applicable to complex $\rho_E(kz_1, k\Delta z)$. However, for general $\rho_E(z_1, z_2)$, the truncation of the numerical integration to finite limits imposes an inherent inaccuracy when ρ_E is not known in closed form. Asymptotic values corresponding to the definition (48) are listed in Table II. Comparison with corresponding values in Table I shows that the anisotropy of the spatial correlation now appears to be usually smaller with this second definition.

Figures 9 and 10 show the dependence of the ratios $\ell^{(\alpha)}(kz_1)/\ell_\infty^{(\alpha)}$ on kz_1 for the transverse, longitudinal, and total fields, for separation in the normal ($\alpha = z$) or tangential ($\alpha = x$) direction, respectively. The definition of $\ell^{(\alpha)}(kz_1)$ that was used in generating these plots is (48). The damped oscillatory dependence of this ratio with increasing kz_1 indicates that the correlation length tends asymptotically to its free-space value, although more slowly for the tangential field than for the normal field. The fluctuations for the total field are significantly smaller and more irregular for tangential separation than for normal separation. Also, the oscillations are significantly stronger for the tangential field than for the normal component. For example, for normal separation at $z_1 = \lambda/2$, this ratio for $E_t(kz_1)$ deviates by more than 25% from the asymptotic value, but by only about 10% for $E_z(kz_1)$.

To verify that the observed oscillatory behavior of $\ell^{(\alpha)}(kz_1)/\ell_\infty^{(\alpha)}$ is not particular to the choice of definition (48), this ratio has also been computed using (47) for normal separation and is shown in Fig. 11. Comparison with Fig. 9 con-

TABLE II. Asymptotic values of correlation length $\ell^{(\alpha)}(kz_1)$ (in units $k\Delta\alpha$) for E_β calculated using (48).

	$\ell^{(z)}(0)$	$\ell^{(z)}(\infty)$	$\ell^{(z)}(0)/\ell^{(z)}(\infty)$	$\ell^{(x)}(0)$	$\ell^{(x)}(\infty)$	$\ell^{(x)}(0)/\ell^{(x)}(\infty)$
E_x	6.38	1.65	3.87	2.29	1.95	1.17
E_y	3.89	1.65	2.35	1.87	1.57	1.19
E_z	2.58	1.88	1.37	1.57	1.57	1.00
E_t	4.35	1.65	2.65			
E	1.38	$\pi/2$	0.88	1.57	$\pi/2$	1.00

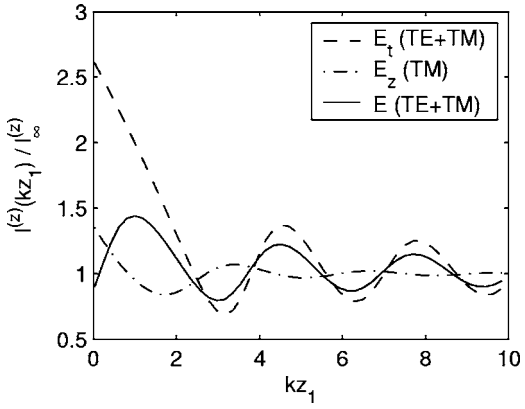

FIG. 9. Normalized correlation distances for separation in normal direction, calculated using (48).

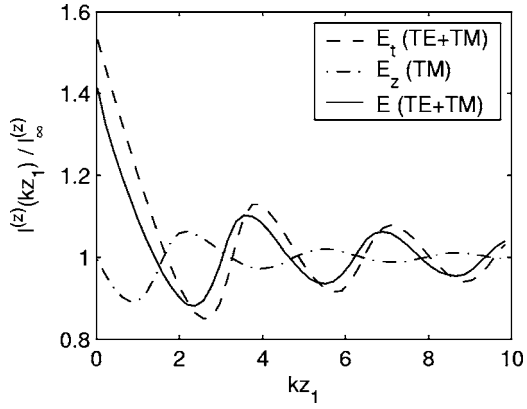

FIG. 11. Normalized correlation distances for separation in normal direction, calculated using (47).

firms that the oscillatory behavior is fundamental and that these two different definitions of $\ell^{(\alpha)}(kz_1)$ for E_t result in mainly quantitative rather than qualitative differences in $\ell^{(z)}(kz_1)/\ell_\infty^{(z)}$. However, for E and to a lesser extent E_z, a considerably larger difference between values for both definitions exists in the close vicinity of the surface. Thus, for *inhomogeneous* random EM fields, the value of the *relative* correlation length depends strongly on the particular choice of definition. This is supplementary to the well-known sensitivity of the absolute correlation length on the choice of definition in the case of homogeneous fields [26]. A general feature is that the correlation length exhibits oscillations as a function of kz_1 that become increasingly more pronounced when $kz_1 \to 0$. These have also been observed in numerical studies of correlation functions inside two-dimensional quantum billiards (Fig. 1 in [6]). Our present result suggests that oscillations of the correlation length around its asymptotic value exist in the presence of a single boundary and, therefore, occur also in open (nonresonant) configurations.

Thus, the following picture emerges, as is illustrated schematically in Fig. 12. [The following discussion is based on values obtained with definition (48).] At arbitrarily large distances from the surface ($kz_1 \to +\infty$), the coherence cell (cf. Sec. VI) is spherically symmetric for the total field E but ellipsoidal for E_x, E_y, and E_z, on account of the different correlation functions for longitudinal vs. transverse components relative to the direction of separation. The respective (dimensionless) coherence volumes of these cells are $\nu_\infty = 2.03$, $\nu_{x,\infty} = \nu_{y,\infty} = 2.66$, and $\nu_{z,\infty} = 2.46$. The major axis of the ellipsoids is along the direction of the field component in question, yielding a prolate spheroid for E_z and an oblate one for E_x or E_y.

When z_1 starts approaching the surface along the normal direction, the shape (axial ratios) and volume of the coherence cells change in a complicated and independent but oscillatory manner, with a quasiperiod of approximately $\lambda/2$. On average, the amplitude of the oscillations and the coherence volume increase in this process. In general, the coherence distances for longitudinal and transverse field components do not change in phase with one another as a function of z_1, whence the coherence cells change shape in a fairly complicated manner. When z_1 reaches the surface, the coherence cells for $E_x^{(x)}$, $E_y^{(x)}$, and $E_z^{(x)}$ are all distinctly prolate in x direction, with respective axial ratios 2.79, 2.08, and 1.63, whereas the originally spherical cell for E is now marginally oblate spheroidal (axial ratio 0.87). The volume of the coherence cells of the field components has increased most prominently for the tangential fields. When using the definition

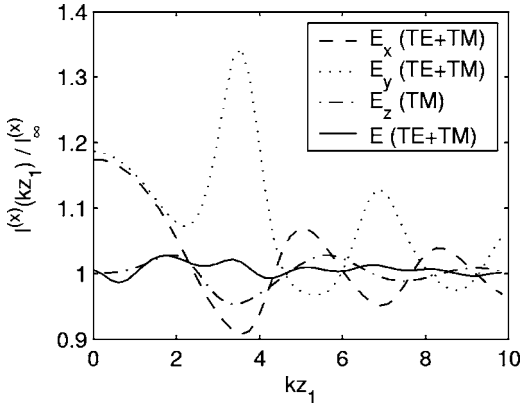

FIG. 10. Normalized correlation distances for separation in tangential direction, calculated using (48).

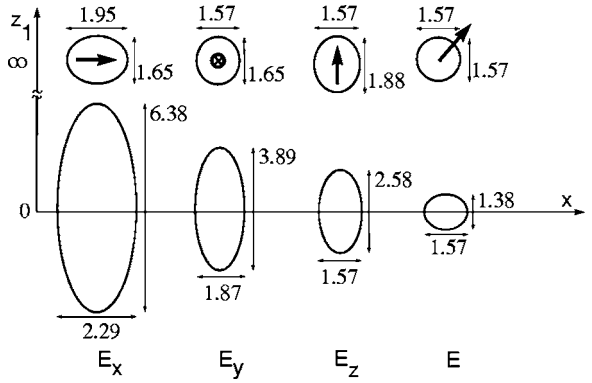

FIG. 12. Correlation cells (ellipsoids) for the electric field and its Cartesian components (directions indicated by arrows) for free random fields ($kz_1 \to +\infty$; top row) and for surface random fields ($kz_1 \to 0$; bottom row). Listed asymptotic values of correlation lengths were calculated based on definition (48) (see Table II).

(47) instead, the dynamics are qualitatively similar but the coherence volumes close to the surface are now significantly larger (typically by a factor between 5 and 10).

VI. DENSITY OF UNCORRELATED POINT LOCATIONS

When estimating sample statistics (e.g., the expected value of the random maximum field amplitude), the local number $N(kz_1)$ of uncorrelated samples is of fundamental interest. For the total field or any component E_β, the ratio

$$\frac{N(kz_1)}{N_\infty(k)} \simeq \frac{\nu_\infty(k)}{\nu(kz_1)}, \tag{49}$$

in which the (dimensionless) volume of the local ellipsoidal coherence cell centered at kz_1 is defined by

$$\nu(kz_1) \triangleq \frac{4\pi}{3}\ell^{(x)}(kz_1)\ell^{(y)}(kz_1)\ell^{(z)}(kz_1), \tag{50}$$

serves as an estimate for the ratio [27] of the number $N(kz_1)$ of volumetrically uncorrelated sampled (point) values contained within an arbitrary physical volume V centered at a distance kz_1 and the corresponding number $N_\infty(k)$ within an equivalent volume but at arbitrarily large distance from the boundary.

The local number $N_\beta(kz_1)$ for $E_\beta(kz_1)$ within V centered around $\mathbf{r}_1$ is then the number of coherence cells contained within $\mathcal{V} \triangleq k^3V$

$$N_\beta(kz_1) \simeq \frac{\mathcal{V}(k)}{\nu_\beta(kz_1)} = \frac{6\pi^2 V}{\lambda^3 \ell^{(x)}_{E_\beta}(kz_1)\ell^{(y)}_{E_\beta}(kz_1)\ell^{(z)}_{E_\beta}(kz_1)} \tag{51}$$

with corresponding point density $n_\beta(kz_1)=k^3/\nu_\beta(kz_1)$.

The value of the ratio (49) is somewhat less sensitive to the particular choice of definition (47) or (48), at least for sufficiently large kz_1, compared to the dependency displayed by the absolute value of the $\ell^{(\alpha)}(kz_1)$ and, hence, (51). This phenomenon has also been observed for homogeneous random EM fields [26].

Specific ratios $N^{(\alpha)}(kz_1)/N^{(\alpha)}_{\beta,\infty}$ for one-dimensional densities may similarly be defined for separations along a specific coordinate direction $\mathbf{1}_\alpha$ (correlation along the line), now with $N^{(\alpha)}_\beta(kz_1) \simeq \mathcal{L}(k)/\nu^{(\alpha)}_\beta(kz_1)$ for a line segment of physical length $L=\mathcal{L}/k$. For an arbitrary spatial linear direction $\mathbf{1}_r$, an effective value can be estimated as

$$\frac{N^{(r)}_\beta(kz_1)}{N^{(r)}_{\beta,\infty}} \simeq \left[\frac{N_\beta(kz_1)}{N_{\beta,\infty}}\right]^{1/3} \tag{52}$$

or, more generally, through elaborated explicit calculation (cf. Sec. IV).

Finally, the effective relative correlation distance as an average value with respect to all spatial directions of separation $\mathbf{1}_r$ can be estimated from (51) as

$$\frac{\ell^{(r)}(kz_1)}{\ell^{(r)}_\infty} \simeq \left[\frac{\nu(kz_1)}{\nu_\infty}\right]^{1/3}. \tag{53}$$

Again, for arbitrary $\mathbf{1}_r$, $\ell^{(r)}(kz_1)$ can be calculated in a more elaborate manner using the method in Sec. IV.

VII. CONCLUSION

In this paper, we derived closed-form expressions for a classical EM random vector field in the presence of an infinite planar PEC surface. For separation of a pair of locations in the direction of the surface normal, the approach of the nearest point toward the surface results in the correlation lengths of the field and its components to increase in value, as witnessed by an increased region of $k\Delta z$ for which the correlation function remains close to unity. For cross-correlation between different and/or mixed field components, the correlation function increases in an oscillatory manner from zero at infinite distance to a large negative value on reaching the surface.

The analysis shows that the correlation distance and, hence, the number of spatially uncorrelated sample points N exhibit fluctuations as a function of the absolute central distance from the wall. Unlike the fluctuations of **E**, however, these are deterministically calculable for the configuration in question. With regard to estimation of sample statistics of **E**, which are based on the value of N, the variability of N leads to increased uncertainties.

ACKNOWLEDGMENT

The author wishes to thank Prof. H. J. Stöckmann for discussions on experimental details relating to Fig. 2(a) of [3].

[1] R. C. Bourret, Nuovo Cimento **18**, 347 (1960).
[2] J. Sarfatt, Nuovo Cimento **27**, 1119 (1963).
[3] B. Eckhardt, U. Dörr, U. Kuhl, and H. J. Stöckmann, Europhys. Lett. **46**, 134 (1999).
[4] C. L. Mehta and E. Wolf, Phys. Rev. **134**, A1143 (1964).
[5] D. A. Hill, IEEE Trans. Electromagn. Compat. **41**, 365 (1999).
[6] A. Bäcker and R. Schubert, J. Phys. A **35**, 539 (2002).
[7] A. Bäcker, R. Fürstberger, R. Schubert, and F. Steiner, J. Phys. A **35**, 10293 (2002).
[8] L. A. Bunimovich, Physica D **33**, 58 (1988).
[9] S. Deus, P. M. Koch, and L. Sirko, Phys. Rev. E **52**, 1146 (1995).
[10] S. Hortikar and M. Srednicki, Phys. Rev. Lett. **80**, 1646 (1998).
[11] A. M. Yaglom, *Correlation Theory of Stationary and Related Random Functions—I. Basic Results* (Springer, Heidelberg, 1987).
[12] R. H. Price, H. T. Davis, and E. P. Wenaas, Phys. Rev. E **48**, 4716 (1993).
[13] W. E. Lamb, Jr., Phys. Rev. **70**, 308 (1946).
[14] J. G. Kostas and B. Boverie, IEEE Trans. Electromagn. Compat. **33**, 366 (1991).
[15] L. R. Arnaut and P. D. West, NPL Report CETM 13 1999, Sec. 3.1.9.

[16] J. M. Dunn, IEEE Trans. Electromagn. Compat. **32**, 53 (1990).
[17] L. R. Arnaut and P. D. West, IEEE Trans. Electromagn. Compat. (to be published).
[18] D. A. Hill, IEEE Trans. Electromagn. Compat. **47**, 281 (2005).
[19] L. R. Arnaut, IEEE Trans. Electromagn. Compat. **44**, 442 (2002); **45**, 568(E) (2003).
[20] M. V. Berry, J. Phys. A **35**, 3025 (2002).
[21] L. R. Arnaut, IEEE Trans. Electromagn. Compat. **47**, 781 (2005).
[22] E. T. Whittaker, Math. Ann. **57**, 333 (1902); specifically Secs. 5.1, 5.2.
[23] E. T. Whittaker and G. N. Watson, *A Course of Modern Analysis*, 4th ed. (Cambridge University Press: Cambridge, UK, 1927), Sec. 18.6, p. 397.
[24] M. V. Berry, J. Phys. A **10**, 2083 (1977).
[25] D. A. Hill and J. M. Ladbury, IEEE Trans. Electromagn. Compat. **44**, 95 (2002).
[26] L. R. Arnaut, IEEE Trans. Electromagn. Compat. **43**, 305 (2001).
[27] The spatial correlation distances vary with the direction of separation and the direction of the field component in question. Note also that $\ell_{E_y}^{(x)} = \ell_{E_x}^{(y)}$.